Histochem Cell Biol (2005) 123: 229–238
DOI 10.1007/s00418-005-0768-3

ORIGINAL PAPER

**Thorsten Wiech · Sylvia Timme · Florian Riede
Stefan Stein · Michael Schuricke · Christoph Cremer
Martin Werner · Michael Hausmann · Axel Walch**

Human archival tissues provide a valuable source for the analysis of spatial genome organization

Accepted: 22 December 2004 / Published online: 13 April 2005

Abstract Sections from archival formalin-fixed, paraffin wax-embedded human tissues are a valuable source for the study of the nuclear architecture of specific tissue types in terms of the three-dimensional spatial positioning and architecture of chromosome territories and sub-chromosomal domains. Chromosome painting, centromeric, and locus-specific probes were hybridized to tissue microarrays prepared from formalin-fixed paraffin wax-embedded samples of pancreas and breast. The cell nuclei were analyzed using quantitative three-dimensional image microscopy. The results obtained from non-neoplastic pancreatic cells of randomly selected individuals indicated that the radial arrangement of the chromosome 8 territories as well as their shape (roundness) did not significantly differ between the individuals and were in accordance with assumptions of a probabilistic model for computer simulations. There were considerable differences between pancreatic tumor and non-neoplastic cells. In non-neoplastic ductal epithelium of the breast there was a larger, but insignificant, variability in the three-dimensional positioning of the centromere 17 and HER2 domains between individuals. In neoplastic epithelial breast cells, however, the distances between centromere and gene domains were, on average, smaller than in non-neoplastic cells. In conclusion, our results demonstrate the feasibility of studying the genome architecture in archival, formalin-fixed, paraffin wax-embedded human tissues, opening new directions in tumor research and cell classification.

T. Wiech · S. Timme · F. Riede
M. Werner (✉) · M. Hausmann · A. Walch
Institute of Pathology,
University Hospital Freiburg,
Albertstraße 19,
79104 Freiburg, Germany
E-mail: dirpath@ukl.uni-freiburg.de
Tel.: +49-761-2036737
Fax: +49-761-2036818

S. Stein · M. Schuricke · C. Cremer
Kirchhoff Institute of Physics,
University of Heidelberg,
Im Neuenheimer Feld 227,
69120 Heidelberg, Germany

Introduction

The linear DNA sequence of genomes exists within the three-dimensional (3D) space of the cell nucleus. Individual chromosomes occupy distinct territories subdivided into subchromosomal domains, differentiated only by less intermingling, and functionally correlated compartments in a hierarchical way (Cremer et al. 2000). The spatial organization of chromosome territories and subchromosomal domains is described in terms of their radial positioning relative to the center of the nucleus, and the arrangement of chromosomes in the interphase nucleus is nonrandom (Cremer and Cremer 2001; Kozubek et al. 2002; Lukásová et al. 2002; Parada and Misteli 2002; Parada et al. 2004b; Zink et al. 2004; Cremer et al. 2004). Chromosomes can be positioned in such a way that gene-dense chromosomes are located preferentially towards the center of the nucleus, whereas gene-poor chromosomes are positioned towards the periphery (Croft et al. 1999; Boyle et al. 2001; Falk et al. 2002; Cremer et al. 2001, 2003). Similar principles are found for the intra-territorial organization of sub-chromosomal domains, e.g., centromeres show a peripheral orientation whereas telomeres or active genes tend to be positioned towards the nuclear center (Amrichová et al. 2003; Weierich et al. 2003). In addition, the centromeres seem to play a significant role in the functional correlation of genome architecture and gene expression (Volpi et al. 2000; Bártová et al. 2002; Taslerová et al. 2003). Remarkably, this radial arrangement has been conserved in lymphocytes over 300 million years of evolution, and has also been reported in fibroblasts, implying functional significance (Tanabe et al. 2002a,

2002b). However, chromosomal gene density appears not to be the only determinant of radial positioning, because in diploid fibroblasts and cultured amniotic fluid cells chromosome size has also been correlated with radial positioning irrespective of the gene density (Sun et al. 2000; Bridger et al. 2000; Cremer et al. 2001). These differences might point to distinct arrangements of chromosomes among cell types and in cells from different tissues.

The nonrandom positioning of chromosomes and genes and the evolutionary conservation of radial chromosome patterns suggest functional relevance (van Driel et al. 2003; Spector 2003). A possible role for spatial genome organization has emerged from comparison of the relative positioning patterns in non-neoplastic and neoplastic cells. The studies suggest that the spatial proximity and compaction of potential translocation partners significantly contributes to their likelihood of undergoing illegitimate rejoining once chromosome breaks have occurred (Lukásová et al. 1999; Neves et al. 1999; Kozubek et al. 1999; Esa et al. 2000; Nikiforová et al. 2000; Parada et al. 2002; Roix et al. 2003). Structural chromosomal aberrations have been described in almost all human cancers, and cytogenetic investigations of neoplastic cells have revealed more than 600 acquired, recurrent, balanced chromosome translocations. Many such genomic rearrangements are cancer-specific and they are valuable diagnostic and prognostic tools. Thus, there might be a possibility of ultimately using aberrant positioning patterns as diagnostic tools, e.g., in predicting tumor risk (Hausmann et al. 2000).

Up to now, higher-order spatial genome organization has mostly been studied in monolayer cultures using tumor cell lines, fibroblast, or lymphocytes (see, e.g., Cremer et al. 2003). Although these cells offer several technical advantages, even "normal" cells in monolayer cultures have a nuclear structure different from that of the same cells in tissues (Lelievre et al. 1998). This complicates comparisons between non-neoplastic (or normal) and neoplastic (or otherwise altered) cell nuclei, and might obscure important points of difference in spatial organization. Thus, the application of approaches allowing the 3D investigation of the genome within the natural context of human tissue would give an insight into addressing the spatial genome organization in both physiological and pathologically altered cells. Currently, sophisticated technologies for the analysis of fluorescence-labeled signals of DNA sequences should reveal new insights into the 3D organization of the genome within various tissues.

Here, we report an approach allowing the assessment of higher-order spatial organization and architecture of chromosome territories, centromere domains, and gene domains in cell nuclei of formalin-fixed and paraffin wax-embedded human tissues. We demonstrate that reliable measurements of radial positioning or shape, described by a roundness parameter of chromosome territories, and centromeric and gene domains, are feasible in cell nuclei within their natural context of normal and neoplastic tissue types from pancreas and breast. In addition, these measurements are compatible with assumptions of a probabilistic model of the organization of the cell nucleus (Kreth et al. 2004).

Materials and methods

Tissues and tissue microarrays

Paraffin wax-embedded human tissue specimens, fixed in buffered formaldehyde (4% in phosphate-buffered saline, PBS), were taken for the preparation of tissue microarrays. These microarrays were designed using two 2-mm tissue cores per tissue specimen taken from the paraffin wax tissue blocks. Morphologically normal and neoplastic (invasive carcinoma) tissue samples of pancreas ($n = 3$ ductal epithelium, $n = 1$ ductal adenocarcinoma, grade 2) and breast ($n = 4$ ductal epithelium, $n = 1$ invasive ductal carcinoma, grade 2) were used. For the analyses, tissue microarray sections (15 μm) were prepared and mounted on glass slides. In each case, the first and last sections were stained with hematoxylin and eosin for histomorphological evaluation.

DNA probe set

Commercially available fluorescence-labeled locus-specific (LSI), centromeric (CEP) and whole chromosome painting (WCP) DNA probes (Abbott Molecular Diagnostics) were applied according to the manufacturer's instructions. The following DNA probes were hybridized on the respective tissues: WCP no. 8 labeled with SpectrumGreen (pancreas, ductal epithelium and ductal adenocarcinoma), LSI Her-2/*neu* labeled with SpectrumOrange, and CEP 17 labeled with SpectrumGreen (breast, ductal epithelium and invasive ductal carcinoma).

Tissue pretreatment, fluorescence in situ hybridization (FISH), and posthybridization washes

Paraffin was removed by xylene for 30 min and isopropanol for 3 min. Then the slides were hydrated over a graded series of ethanol (100%, 96%, 70%, and 50%) and PBS (pH 7). The tissue was pretreated by heating the slides for 20 min in a microwave oven (180 W) in citrate buffer (pH 7) followed by pronase E (0.05%) digestion for 3 min at 37°C. After washing three times for 3 min with PBS (pH 7), the slides were denatured in 70% formamide and 2× standard saline citrate (SSC), pH 7, for 15 min at 73°C. Before in situ hybridization, the slides were dehydrated over a graded series of ethanol (70%, 90%, 100%, at −20°C) and air dried. The fluorescence-labeled DNA probes were added to the pretreated slides according to the manufacturer's

instructions and incubated for 48 h at 37°C. After in situ hybridization, the slides were placed in 2× SSC/0.1% NP-40 (pH 7.4) at 73°C for 2 min and then embedded with an antifade solution (Vectashield) after incubating with 4',6-diamidino-2-phenylindole (DAPI) as nuclear counterstain. For microscopy the slides were covered with a standard cover glass.

Fluorescence microscopy and 3D image acquisition

Fluorescence images of FISH-labeled nuclei from tissue cells were acquired with a Zeiss Axioplan2 imaging microscope (Carl Zeiss Jena, Jena, Germany) equipped with a PlanApochromat ×100/NA1.4 oil objective lens (analysis of pancreatic cells) or a PlanApochromat ×63/NA1.4 oil objective lens (analysis of breast cells) and appropriate filter settings for DAPI, SpectrumGreen (FITC), and SpectrumOrange illumination and detection. For optical sectioning through the specimens, the recently developed ApoTome (Carl Zeiss Jena) was implemented into the microscopic setup. The images were recorded by means of an AxioCam b/w CCD camera (Carl Zeiss Jena). The complete setup was computer controlled by the AxioVision software (Carl Zeiss Jena) running under Windows 2000 on a PC (Hausmann et al. 2004). For 3D imaging, optical sectioning was performed. The image stacks typically consisted of 20–40 image slices with a pixel size of 65×65 nm (×100 objective) or 102×102 nm (×63 objective) and a z distance of 325–350 nm. This was enough to fulfill the Nyquist image acquisition theorem. The image sections were further processed by the AxioVision software and reconstructed into a 3D view in false colors. In addition, the image stacks were exported as tiff-image series for further quantitative evaluation.

Image segmentation and quantitative evaluation

From these digitized data sets, cell nuclei were selected interactively and optically isolated from the surrounding tissue by visual inspection using the image processing program ImageJ. This additional step of presegmentation was usually necessary to avoid misinterpretation due to overlapping or closely attached cell nuclei.

For further processing, the data were converted into kdf-image format and evaluated using home-developed program packages running under Linux 8.0 (SuSE Linux) on a PC (for a detailed description of the quantitative radial 3D evaluation by a voxel-based algorithm, see Cremer et al. 2001; a detailed description of the complete software package for threshold independent analyses of geometric parameters will be published elsewhere; Stein et al. manuscript in preparation).

In brief, the images were processed with a background subtractor and a weak Gaussian filter to reduce nonspecific artifacts, staining background, and detection noise. The center of gravity and the border of the nucleus were automatically determined using the 3D image stack of the counterstain. All voxels below an automatically calculated threshold were set to zero and belonged to the background. In order to compare nuclei of different shapes and sizes, the distance between the nuclear center and each point on the segmented nuclear border was normalized to the relative radius $r_0 = 100$. In the same way, the segmentation of the labeled genome region (chromosome territory, centromere domain, gene domain) was performed in each 3D data stack representing the respective color channels. The segmented nuclear space was divided into 25 equidistant shells with a thickness of $\Delta r = r_0/25$. For each of these shells, all voxels ($r_{\text{shell}} - \Delta r/2 < r_{\text{voxel}} \leq r_{\text{shell}} + \Delta r/2$) assigned to a given labeled genome region were identified and their fluorescence intensities were summed. For each evaluated nucleus, this procedure yielded the specific DNA shell content. Finally, the sum of the voxel intensities measured in all evaluated nuclei (typically 20–40 per set) was set to 100% for each color channel. With this normalization, the DNA content in the nuclear shells was plotted as a function of the relative distance r from the 3D center of gravity of the nucleus. From these curves, the localization of the genome regions was determined by the mean value of r at the third quartile.

For further image analysis, a software package that quantifies geometric data such as numbers, volumes, surfaces, shapes, or distances of labeled genome regions over a reasonable threshold spectrum was used (Stein et al. 2004). Here, the parameters volume, surface, and roundness were used to characterize the labeled chromosome 8 territories in pancreatic cell nuclei. In brief, the cell nucleus and the chromosome territories inside the nucleus were segmented starting at a given threshold value. A voxel belonging to a chromosome territory was defined by a 26 neighborhood, meaning that all 26 voxels in the neighborhood of the current central voxel belong to the object. After segmentation all parameters (volume, surface, roundness) were calculated and the mean values of all segmented chromosome territories were stored in the list of results. Then the segmentation threshold was increased in discrete steps up to the highest value and the procedure was repeated for each threshold. With one cycle of the program one cell nucleus was analyzed for the complete threshold spectrum. For the analysis of a large number of cell nuclei, this algorithm was implemented into a script. Finally, the average and the standard deviation of the mean of the parameters for all cell nuclei of a data set were calculated and stored in an ASCII file and plotted against the threshold values. In order to compare image sets of different signal-to-noise ratios, the volume and surface data were normalized, with a maximum of 1.

Volume, surface, and roundness of chromosome territories were calculated independently from the voxel intensity. This means that the voxel number or the number of voxel surfaces were part of the calculation formula. With d x being the lateral voxel size and d z being the axial voxel size, the territory volume V, surface S, and roundness R for a certain threshold were given by

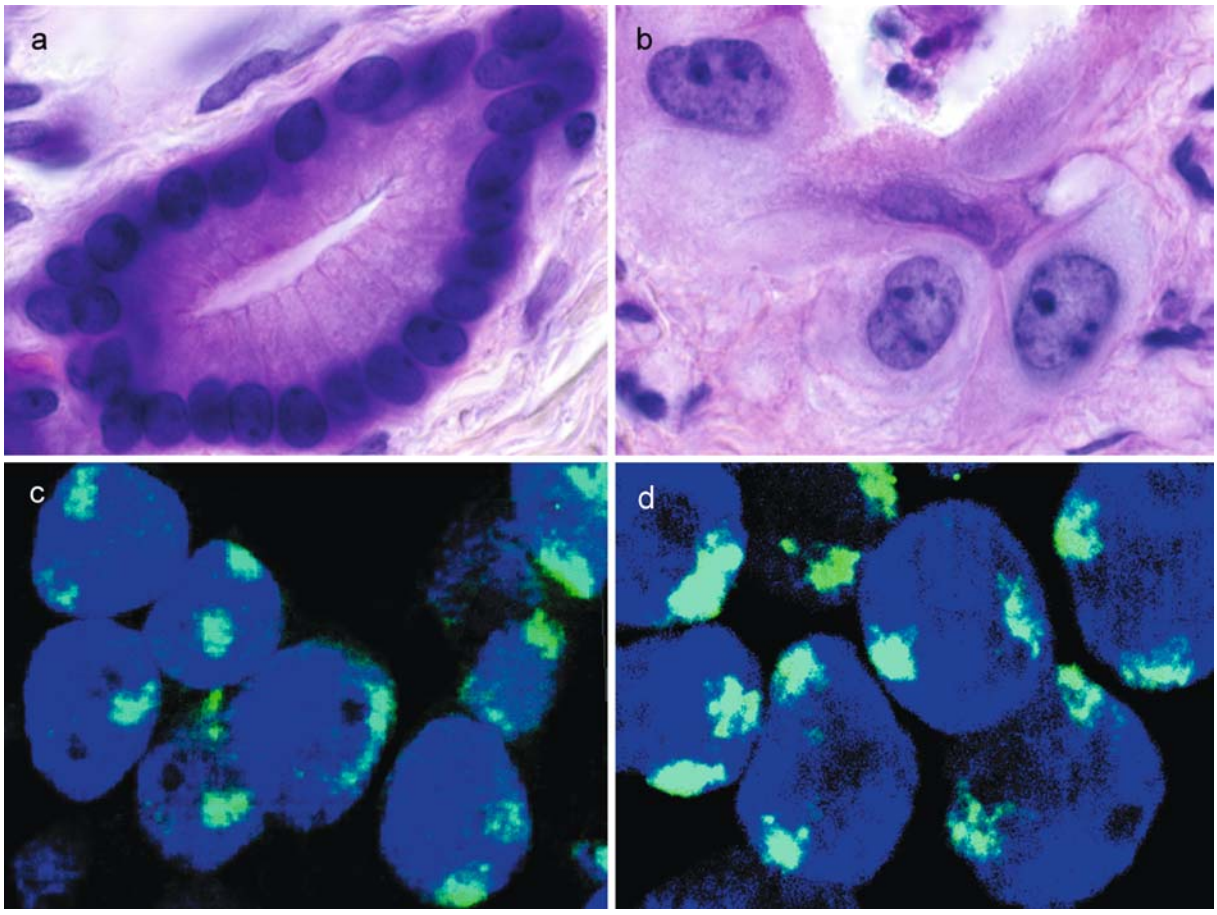

Fig. 1 **a**, **b** Microphotographs (×100) of (**a**) non-neoplastic epithelium of a pancreatic duct and (**b**) an associated invasive adenocarcinoma (hematoxylin and eosin). **c**, **d** Fluorescence images of the same tissue hybridized with whole chromosome painting probe 8 (*green territories*) showing DAPI-stained interphase cell nuclei of (**c**) non-neoplastic epithelium of a pancreatic duct and (**d**) invasive adenocarcinoma

$$V = 1/n \sum n(m_n \mathrm{d}x^2 \mathrm{d}z),$$
$$S = 1/n \sum n(k_n \mathrm{d}x^2 + I_n \mathrm{d}x\, \mathrm{d}z),$$
$$R = 36\pi(V^2/S^3)$$

with n is the number of territories, m_n the number of voxels in the territory n, and k_n (l_n) the number of lateral (axial) surfaces of the territory n.

Statistical analysis

To test for statistically significant differences in the distribution curves, two tests were applied. The volume, surface, and roundness curves were tested by the Mann–Whitney *U*-test (Altmann 1991). This test is an alternative to the independent group *t*-test, when the assumption of normality or equality of variance is not met. For comparison of the radial distributions, the more stringent, double-sided Kolmogorov–Smirnov test (Knuth 1981) was applied.

Results

Pancreatic tissue (ductal epithelium and invasive ductal adenocarcinoma, chromosome 8)

Images of non-neoplastic cell nuclei obtained from three different individuals were quantitatively analyzed in terms of the 3D radial positioning of the chromosome territories and their roundness (Figs. 1 and 2). Although the three tissue specimens were randomly selected, a very high level of coincidence was found for both parameters. With the double-sided Kolmogorov–Smirnov test no significant difference between each pair of radial distribution curves was found for the three levels of significance tested (Table 1). Also according to the Mann–Whitney test, no significant differences were found in the average shape of the chromosomes described by the roundness (Table 2), a parameter that describes the elongation of the territory (a roundness value of 1 indicates an ideal 3D ball; values of < 1 indicate an ellipsoidal shape).

Radial positioning of the chromosome territories 8 was also compared to recently published model simulations (Kreth et al. 2004). For this purpose, the position of the chromosome was defined by the mean *r*-value at the third quartile. These mean data varied between 64 and 68 with an average of 67 ± 2, which agreed well with

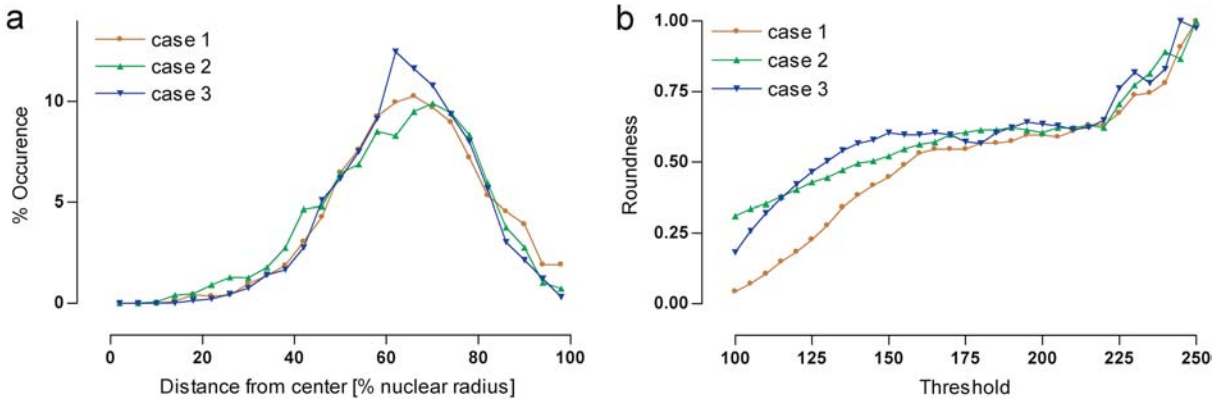

Fig. 2 Quantitative 3D evaluation of interphase cell nuclei derived from non-neoplastic epithelium of pancreatic ducts of tissue from three individuals. **a** Relative DNA content of chromosome territory 8 versus normalized radius. **b** Roundness versus segmentation threshold (for details see Materials and methods)

the computer simulation of the suggested probabilistic model, where values between 67 and 76 were calculated for chromosome 8.

In conclusion, these results indicate a high degree of conservation of the nuclear architecture between different individuals under normal, i.e., non-neoplastic, cellular conditions.

In order to determine the influence of neoplastic transformation of cell nuclei on the genome architecture, we compared carcinoma cells with non-neoplastic cells in one case in terms of 3D radial distribution, normalized volume and surface, and roundness (Fig. 3). A slight difference in the radial position, which was significant at $P < 0.05$ according to the Kolmogorov–Smirnov test, was detected. In contrast, no significant differences were found for the normalized volume and surface using the Mann–Whitney *U*-test (Table 3). The roundness curves, however, differed significantly for all *P*-values ($P < 0.1$ to $P < 0.001$) tested. This result suggests that neoplastic transformation of cell nuclei may be correlated primarily to a modification of the shape of the chromosome territory 8. The radial shift of the territory position may be a consequence of this modification by shifting the territory center of gravity.

Table 1 Results of the double-sided Kolmogorov Smirnov test for radial positioning of chromosome 8 territories in cell nuclei derived from non-neoplastic epithelium of pancreatic ducts (see Fig. 2), and centromere 17 and Her2 domains in cell nuclei derived from non-neoplastic terminal ductal epithelium of the breast (see Fig. 5). The symbols +/− mean that the cell nuclei do/do not contain significantly different entities

	$P < 0.1$	$P < 0.075$	$P < 0.05$
Chromosome 8 territories (pancreas)			
Case 1 vs case 2	−	−	−
Case 1 vs case 3	−	−	−
Case 2 vs case 3	−	−	−
Centromere 17 domains (breast)			
Case 1 vs case 2	+	+	−
Case 1 vs case 3	+	+	−
Case 1 vs case 4	−	−	−
Case 2 vs case 3	−	−	−
Case 2 vs case 4	−	−	−
Case 3 vs case 4	−	−	−
Her2 gene domains (breast)			
Case 1 vs case 2	−	−	−
Case 1 vs case 3	−	−	−
Case 1 vs case 4	−	−	−
Case 2 vs case 3	−	−	−
Case 2 vs case 4	−	−	−
Case 3 vs case 4	−	−	−

Breast tissue (ductal epithelium and invasive-ductal carcinoma, centromere 17, HER2)

Images of non-neoplastic cell nuclei obtained from four different individuals were quantitatively analyzed in terms of the 3D radial positioning of the centromere domains and the gene domains (Figs. 4 and 5). Although the data showed a larger variability between the four individuals as compared to the chromosome 8 territories in pancreatic ductal epithelium, again a high level of coincidence was found for both labeled regions (Table 1).

In addition, however, tumor cells showed on average smaller distances between centromere and gene

Table 2 Results of the Mann–Whitney *U*-test for the roundness of chromosome 8 territories in cell nuclei derived from non-neoplastic epithelium of pancreatic ducts (see Fig. 2). The symbols +/− mean that the cell nuclei do/do not contain significantly different entities

Roundness	*z*-value	$P < 0.1$	$P < 0.05$	$P < 0.02$	$P < 0.01$	$P < 0.001$
Case 1 vs case 2	1.3450	−	−	−	−	−
Case 1 vs case 3	1.8799	+	−	−	−	−
Case 2 vs case 3	0.4859	−	−	−	−	−

domains in than non-neoplastic cells (Fig. 6). For the non-neoplastic cell nuclei analyzed, the HER2 domain was on average positioned at $r = 46 \pm 5$ and the centromere 17 domain at $r = 72 \pm 5$, whereas the same domains were positioned in the tumor cell nuclei at 44 and 62.

Finally, the radial positioning of chromosome 17 was also compared to that in recently published model simulations (Kreth et al. 2004). For this purpose, the positions of the centromere domains and the HER2 domains were summed to represent the chromosome. The mean position was calculated to lie at $r = 59 \pm 14$. Under the assumption that our experimental data did not cover the whole chromosome territory and thus showed a shift of the center of gravity to the periphery of the nucleus, this could agree with the computer simulation of the suggested probabilistic organization model of the cell nucleus, where *r*-values between 21 and 47 were calculated for chromosome 17. The differences may, however, also have been due to a tissue-specific arrangement of chromosome territories, which has been suggested in Cremer et al. (2003).

Fig. 3 Quantitative 3D evaluation of interphase cell nuclei derived from non-neoplastic epithelium of pancreatic ducts and associated invasive adenocarcinoma of an individual. **a** Relative DNA content of chromosome territory 8 versus normalized radius. **b** Roundness versus segmentation threshold. **c** Normalized volume versus segmentation threshold. **d** Normalized surface versus segmentation threshold (for details see Materials and methods)

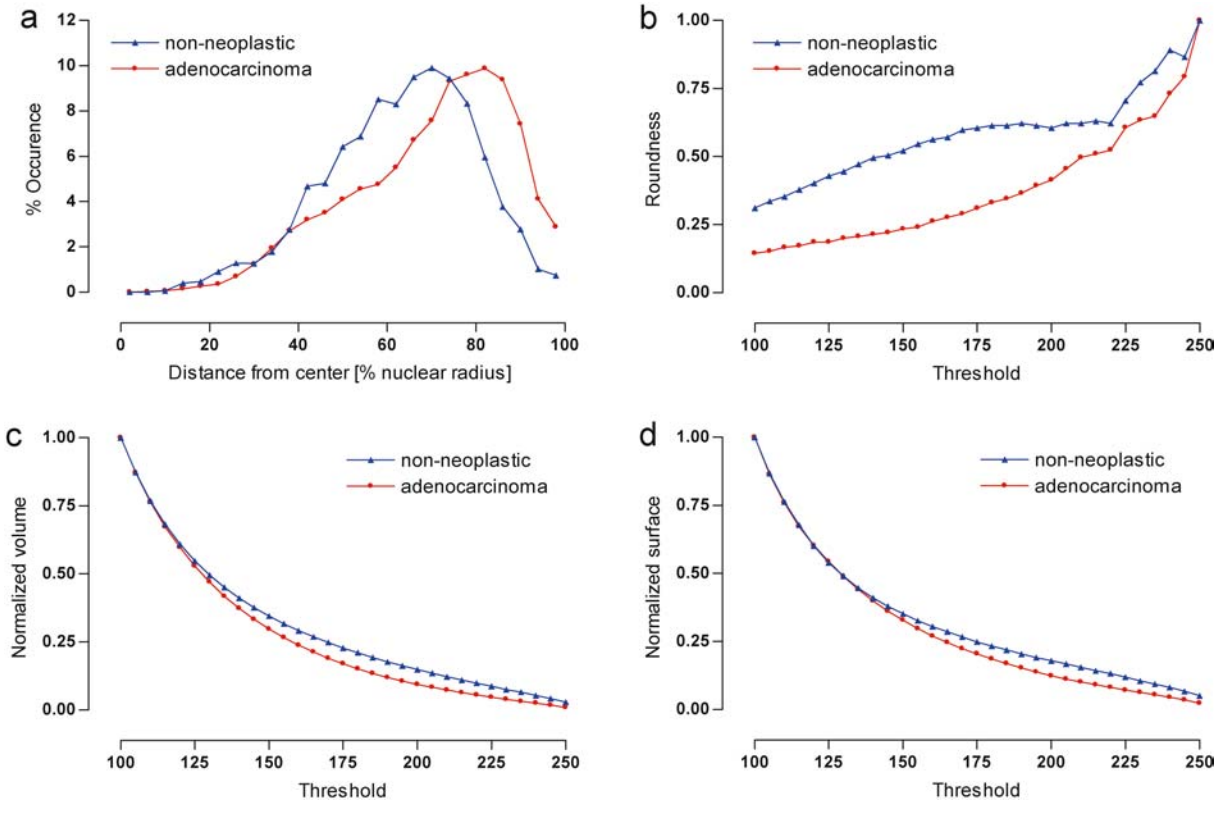

Discussion

In this report, a new approach to the study of the genome architecture in cell nuclei within their histological context obtained from archival, formalin-fixed, paraffin wax-embedded tissue blocks is presented. Our results obtained from the ductal epithelium of pancreas indicate that the radial arrangement of chromosome territories, as well as their shape described by the roundness of the territories, do not significantly differ between randomly selected individuals and are in good accordance with assumptions from adopting a probabilistic model for computer simulations of the nuclear organization (Kreth et al. 2004). In contrast, the comparison of tumor and non-neoplastic cells suggested considerable differences in chromosome positioning and genome architecture.

Studies of the higher-order chromatin architecture at the light microscope level (i.e., in the order of the microscale) require 3D-FISH protocols that maintained the shape and 3D structure of the nuclei as well as possible. The tissues analyzed in the present study were fixed in a buffered 4% formaldehyde solution, which has been recommended particularly for 3D preservation (Cremer et al. 2004). To enable sufficient DNA probe penetration during in situ hybridization in formalin-fixed tissue sections, we pretreated the sections with heat and pronase E to provide a feasible compromise between optimal penetration of probe DNA into the cell nucleus, little nonspecific fluorescence background, and structural preservation of the genome microarchitecture (Walch et al. 2001). An important factor for systematic

Table 3 Results of the Mann–Whitney *U*-test for shape parameters of chromosome 8 territories in neoplastic versus non-neoplastic pancreatic cell nuclei of case 2 (see Fig. 3). The symbols +/− mean that the cell nuclei do/do not contain significantly different entities

	z-value	$P < 0.1$	$P < 0.05$	$P < 0.02$	$P < 0.01$	$P < 0.001$
Normalized volume	0.922	−	−	−	−	−
Normalized surface	1.056	−	−	−	−	−
Roundness	3.915	+	+	+	+	+

investigations of intraindividual and interindividual changes in the nuclear architecture is the reliability of 3D-FISH experiments to assess the 3D positions of chromosome territories down to the level of chromatin domains of about 1 Mb, as well as other nuclear structures. A previous study by Solovei et al. (2002) compared the intranuclear distribution of H2B-GFP-tagged chromatin and the positions of replication-labeled chromatin domains in the same individual cells in vivo, after fixation with 4% formaldehyde, and after 3D FISH. The authors found a high degree of preservation of the spatial arrangement of chromatin domains of about 1 Mb, supporting the reliability of 3D-FISH experiments in the analysis of the topology of formaldehyde-fixed cell nuclei (Solovei et al. 2002).

So far, higher-order spatial genome organization has mostly been studied in monolayer cultures using tumor cell lines, fibroblasts, or lymphocytes (see, for example, Cremer et al. 2001, 2003). These cells offer the advantage of easy growth, observation, and manipulation. Even "normal" cells in monolayer cultures, however, have a nuclear structure different from that of the same cells in tissues (Lelievre et al. 1998). This complicates comparisons between normal and neoplastic (or otherwise altered) cell nuclei, and might obscure important points of difference in spatial genome organization. Therefore, the data derived from cell nuclei in their natural histological context as presented here provide an insight into the spatial genome organization in both physiological and pathologically altered cells in human tissue samples. Recently, Parada et al. (2004a) have provided evidence for tissue-specific spatial organization of genomes in isolated interphase cell nuclei obtained from kidney, liver, and lung tissues of C57BL/6 mice. While Parada et al. (2004a) demonstrated that chromosomes are distributed in a tissue-specific way with respect to their position relative to the center of the nucleus and also

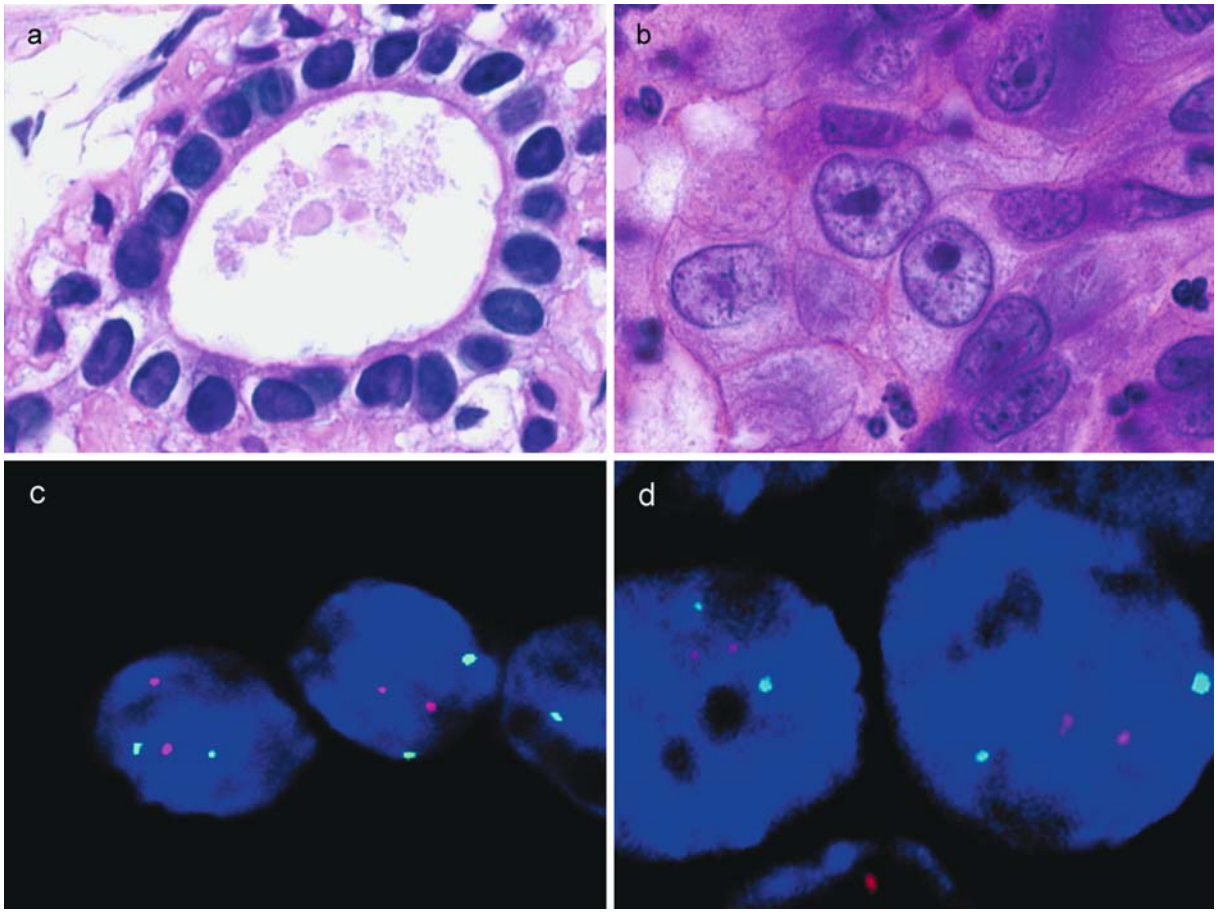

Fig. 4 **a**, **b** Microphotographs (×100) of (**a**) non-neoplastic terminal ductal epithelium of the breast and (**b**) an associated invasive ductal carcinoma (hematoxylin and eosin). **c**, **d** Fluorescence images of the same tissue simultaneously hybridized with a locus-specific DNA probe for HER2 (*red signals*) and a DNA probe for centromere 17 (*green signals*) in DAPI-stained interphase cell nuclei of (**c**) non-neoplastic terminal ductal epithelium of the breast and (**d**) an associated invasive ductal carcinoma

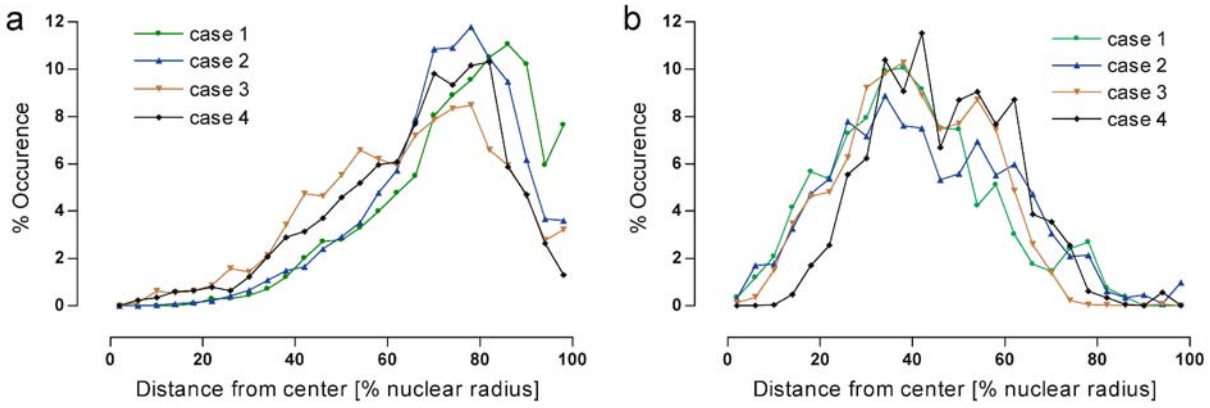

Fig. 5 Quantitative 3D evaluation of interphase cell nuclei derived from non-neoplastic terminal ductal epithelium of the breast from four individuals. **a** Relative DNA content of centromere 17 domain versus normalized radius. **b** Relative DNA content of HER2 domain versus normalized radius (for details see Materials and methods)

relative to each other, it remains unclear whether there are interindividual variations.

Our results derived from non-neoplastic cells of randomly selected human individuals indicate that the radial arrangement of gene domains and chromosome territories, as well as the shape described by the roundness of the territories, do not significantly differ between the individuals and are in good accordance with assumptions from adopting a probabilistic model for chromosome positioning. This probabilistic positioning code has also been found for lymphocyte cell nuclei (Kreth et al. 2004). Thus, our results indicate a high degree of conservation of the nuclear architecture between different individuals under normal, i.e. non-neoplastic, cellular conditions.

The comparison of pancreatic neoplastic (''tumor'') and non-neoplastic (''normal'') cells described here indicated only a slight difference in radial positioning of chromosome 8 ($P < 0.05$; Kolmogorov–Smirnov test). This observation is in agreement with previous reports. Cremer et al. (2003) found maintenance of chromosome territories 18 and 19 in normal and tumor cell nuclei of several tumor cell lines. The maintenance of a radial arrangement of different genetic domains in normal and leukemic blood cells has also been reported by Kozubek et al. (2002). In contrast to radial positioning, the roundness curves of chromosome 8, however, differed significantly. This result could indicate that neoplastic transformation of cell nuclei is correlated primarily to a modification of the shape of the chromosome territory 8. The radial shift of the position of the territory may be a consequence of this modification by shifting the territory center of gravity.

Our observations might also point to tumor-specific changes in spatial genome organization of neoplastic cell nuclei compared with their non-neoplastic counterparts in the same tissues of a given patient. As previously reported, differences in chromosome positioning are not due to variation in cell size or shape among tissues (Cremer et al. 2001). Furthermore, although changes in chromosome positioning have been reported for the G_0/G_1 transition, our observed differences are unlikely to be due to cell cycle effects, as radial chromosome positioning does not significantly change during interphase in cycling cells (Bridger et al. 2000; Walter et al. 2003; Gerlich et al. 2003). While we show here for a limited subset of chromosomes a differential spatial organization, we suspect that these changes are general features

Fig. 6 Quantitative 3D evaluation of interphase cell nuclei of the breast. Relative DNA content of centromere 17 domain (*green*) and HER2 domain (*red*) versus normalized radius. **a** Interphase cell nuclei derived from non-neoplastic terminal duct epithelium of the breast. **b** Interphase cell nuclei derived from invasive-ductal carcinoma (for details see Materials and methods)

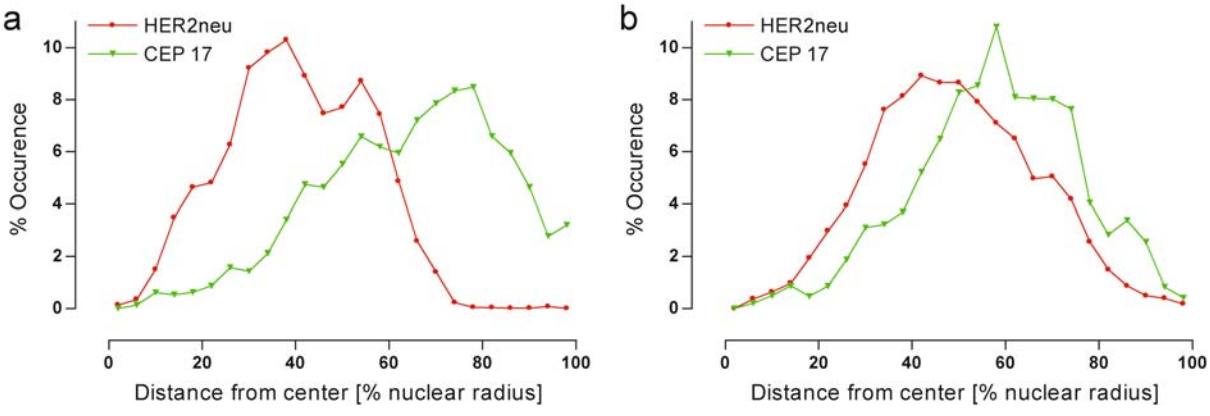

of most chromosomes and genes in various diseased human tissue types. Regardless of the patterns of changes reported here for pancreatic and breast cancer cell nuclei, our description of tissue-specific spatial genome changes should be of use in further experimental tests of these tumor types as well as in understanding the functions and mechanisms of nonrandom spatial genome organization. This may be achieved by a combination of 3D interphase cytogenetics as described here and gene or protein expression analysis obtained from the very same tissue sample of a given patient. In particular, it might be possible to identify recurrent changes in spatial genome organization which predict disease development and progression. The potential applications of our approach to archival tissues include the elucidation of the spatial order of the genome in variably differentiated cell types of normal tissues and the analysis of pathological processes such as the transition from precancerous lesions to invasive and metastatic cancer.

In conclusion, our results demonstrate the feasibility of studying the genome architecture in archival, formalin-fixed, paraffin wax-embedded human tissues, which will open new directions in tumor research and novel aspects concerning supramolecular features in cell classification.

Acknowledgements The authors thank L. Bokla, Freiburg, for excellent technical assistance. The authors gratefully acknowledge the financial support of the Deutsche Krebshilfe (AZ: 79–2789-Si 3) and the Bundesminister für Bildung und Forschung (FKZ 13N8350).

References

Altmann DG (1991) Practical statistics for medical research. Chapman and Hall, London, pp 194–197

Amrichová J, Lukášová E, Kozubek S, Kozubek M (2003) Nuclear and territorial topography of chromosome telomeres in human lymphocytes. Exp Cell Res 289:11–26

Bártová E, Kozubek S, Jirsová P, Kozubek M, Gajová H, Lukásová E, Skalniková M, Ganová A, Koutná I, Hausmann M (2002) Nuclear topography and gene activity in human differentiated cells. J Struct Biol 139:76–89

Boyle S, Gilchrist S, Bridger JM, Mahy NL, Ellis JA, Bickmore WA (2001) The spatial organization of human chromosomes within the nuclei of normal and emerin-mutant cells. Hum Mol Genet 10:211–219

Bridger JM, Boyle S, Kill IR, Bickmore WA (2000) Re-modelling of nuclear architecture in quiescent and senescent human fibroblasts. Curr Biol 10:149–152

Cremer M, Hase J von, Volm T, Brero A, Kreth G, Walter J, Fischer C, Solovei I, Cremer C, Cremer T (2001) Non-random radial higher-order chromatin arrangements in nuclei of diploid human cells. Chromos Res 9:541–567

Cremer M, Küpper K, Wagler B, Wizelman L, Hase J von, Weiland Y, Kreja L, Diebold J, Speicher MR, Cremer T (2003) Inheritance of gene density-related higher order chromatin arrangements in normal and tumor cell nuclei. J Cell Biol 162:809–820

Cremer T, Cremer C (2001) Chromosome territories, nuclear architecture and gene regulation in mammalian cells. Nat Rev Genet 2:292–301

Cremer T, Kreth G, Koester H, Fink RHA, Heintzmann R, Cremer M, Solovei I, Zink D, Cremer C (2000) Chromosome territories, inter chromatin domain compartment and nuclear matrix: an integrated view on the functional nuclear architecture. Crit Rev Eukaryot Gene Expr 10:179–212

Cremer T, Kupper K, Dietzel S, Fakan S (2004) Higher order chromatin architecture in the cell nucleus: on the way from structure to function. Biol Cell 96:555–567

Croft JA, Bridger JM, Boyle S, Perry P, Teague P, Bickmore WA (1999) Differences in the localization and morphology of chromosomes in the human nucleus. J Cell Biol 145:1119–1131

van Driel R, Fransz PF, Verschure PJ (2003) The eukaryotic genome: a system regulated at different hierarchical levels. J Cell Sci 116:4067–4075

Esa A, Edelmann P, Trakhtenbrot L, Amariglio N, Rechavi G, Hausmann M, Cremer C (2000) 3D-Spectral Precision Distance Microscopy (SPDM) of chromatin nanostructures after triple-colour DNA labelling: a study of the BCR-region on chromosome 22 and the Philadelphia chromosome. J Microsc 199:96–105

Falk M, Lukásová E, Kozubek S, Kozubek M (2002) Topography of genetic elements of X-chromosome relative to the cell nucleus and to the chromosome X territory determined for human lymphocytes. Gene 292:13–24

Gerlich D, Beaudouin J, Kalbfuss B, Daigle N, Eils R, Ellenberg J (2003) Global chromosome positions are transmitted through mitosis in mammalian cells. Cell 112:751–764

Hausmann M, Esa A, Edelmann P, Trakhtenbrot L, Amariglio N, Rechavi G, Cremer C (2000) Einblicke in die dreidimensionale Architektur des Zellkerns. In: Heinemann G, Müller WU (eds) Strahlenbiologie und Strahlenschutz—Individuelle Strahlenempfindlichkeit und ihre Bedeutung für den Strahlenschutz, vol. I. TÜV-Verlag, Cologne, pp 87–104

Hausmann M, Cremer C, Linares-Cruz G, Nebe TC, Peters K, Plesch A, Tham J, Vetter M, Werner M (2004) Standardisation of FISH-procedures: summary of the second discussion workshop. Cell Oncol 26:119–124

Knuth DE (1981) The art of computer programming. Addison, Reading, UK

Kozubek S, Lukášová E, Mareckova A, Skalniková M, Kozubek M, Bartová E, Kroha V, Krahulcová E, Slotová J (1999) The topological organization of chromosomes 9 and 22 in cell nuclei has a determinative role in the induction of t(9,22) translocations and in the pathogenesis of t(9,22) leukemias. Chromosoma 108:426–435

Kozubek S, Lukášová E, Jirsová P, Koutná I, Kozubek M, Ganová A, Bártová E, Falk M, Paseková R (2002) 3D structure of the human genome: order in randomness. Chromosoma 111:321–331

Kreth G, Finsterle J, Hase J von, Cremer M, Cremer C (2004) Radial arrangement of chromosome territories in human cell nuclei: a computer model approach based on gene density indicated a probabilistic global positioning code. Biophys J 86:2803–2812

Lelievre SA, Weaver VM, Nickerson JA, Larabell CA, Bhaumik A, Petersen OW, Bissell MJ (1998) Tissue phenotype depends on reciprocal interactions between the extracellular matrix and the structural organization of the nucleus. Proc Natl Acad Sci U S A 95:14711–14716

Lukášová E, Kozubek S, Kozubek M, Kjeronská J, Rýznar L, Horáková J, Krahulcová E, Horneck G (1999) Localisation and distance between ABL and BCR genes in interphase nuclei of bone marrow cells of control donors and patients with chronic myeloid leukaemia. Hum Genet 100:525–535

Lukášová E, Kozubek S, Kozubek M, Falk M, Amrichová J (2002) The 3D structure of human chromosomes in cell nuclei. Chromos Res 10:535–548

Neves H, Ramos C, da Silva MG, Parreira A, Parreira L (1999) The nuclear topography of ABL, BCR, PML, and RARalpha genes: evidence for gene proximity in specific phases of the cell cycle and stages of hematopoietic differentiation. Blood 93:1197–1207

Nikiforova MN, Stringer JR, Blough R, Medvedovic M, Fagin JA, Nikiforov YE (2000) Proximity of chromosomal loci that par-

ticipate in radiation-induced rearrangements in human cells. Science 290:138–141
Parada L, Misteli T (2002) Chromosome positioning in the interphase nucleus. Trends Cell Biol 12:425–432
Parada LA, McQueen PG, Munson PJ, Misteli T (2002) Conservation of relative chromosome positioning in normal and cancer cells. Curr Biol 12:1692–1697
Parada LA, McQueen PG, Misteli T (2004a) Tissue specific spatial organization of genomes. Genome Biol 5:R44. Epub 21 Jun 2004
Parada LA, Sotiriou S, Misteli T (2004b) Spatial genome organization. Exp Cell Res 296:64–70
Roix JJ, McQueen PG, Munson PJ, Parada LA, Misteli T (2003) Spatial proximity of translocation-prone gene loci in human lymphomas. Nat Genet 34:287–291
Solovei I, Cavallo A, Schermelleh L, Jaunin F, Scasselati C, Cmarko D, Cremer C, Fakan S, Cremer T (2002) Spatial preservation of nuclear chromatin architecture during three-dimensional fluorescence in situ hybridization (3D-FISH). Exp Cell Res 276:10–23
Spector DL (2003) The dynamics of chromosome organization and gene regulation. Annu Rev Biochem 72:573–608
Stein S, Solovei I, Cremer M, Zinner R, Timme S, Walch A, Werner M, Hausmann M, Cremer C (2004) 3D-image analysis of the topological organisation of chromatin in human lymphocytes, fibroblasts and in cancer cells of formalin-fixed, paraffin-embedded tissue sections. 15th International Chromosome Conference, London, 5–10 September 2004. Chromos Res 12 [Suppl 1]:34
Sun HB, Shen J, Yokota H (2000) Size-dependent positioning of human chromosomes in interphase nuclei. Biophys J 79:184–190
Tanabe H, Habermann FA, Solovei I, Cremer M, Cremer T (2002a) Non-random radial arrangements of interphase chromosome territories: evolutionary considerations and functional implications. Mutat Res 504:37–45
Tanabe H, Muller S, Neusser M, Hase J von, Calcagno E, Cremer M, Solovei I, Cremer C, Cremer T (2002b) Evolutionary conservation of chromosome territory arrangements in cell nuclei from higher primates. Proc Natl Acad Sci U S A 99:4424–4429
Taslerová R, Kozubek S, Lukásová E, Jirsová P, Bártová E, Kozubek M (2003) Arrangement of chromosome 11 and 22 territories, EWSR1 and FLI1 genes, and other genetic elements of these chromosomes in human lymphocytes and Ewing sarcoma cells. Hum Genet 112:143–155
Volpi EV, Chevret E, Jones T, Vatcheva R, Williamson J, Beck S, Campbell RD, Goldworthy M, Powis SH, Ragoussis J, Trowsdale J, Sheer D (2000) Large-scale chromatin organization of the major histocompatibility complex and other regions of human chromosome 6 and its response to interferon in interphase nuclei. J Cell Sci 113:1565–1576
Walch A, Bink K, Hutzler P, Böwering K, Letsiou I, Zitzelsberger H, Braselmann H, Stein H, Höfler H, Werner M (2001) Sequential multilocus fluorescence in situ hybridization can detect complex patterns of increased gene dosage at the single cell level in tissue sections. Lab Invest 81:1457–1459
Walter J, Schermelleh L, Cremer M, Tashiro S, Cremer T (2003) Chromosome order in HeLa cells changes during mitosis and early G1, but is stably maintained during subsequent interphase stages. J Cell Biol 160:685–697
Weierich C, Brero A, Stein S, Hase J von, Cremer C, Cremer T, Solovei I (2003) Three-dimensional arrangements of centromeres and telomeres in nuclei of human and murine lymphocytes. Chromos Res 11:485–502
Zink D, Fischer AH, Nickerson JA (2004) Nuclear structure in cancer cells. Nat Rev Cancer 4:677–687